

307

~~CONFIDENTIAL~~

Copy
RM L53K12

NACA RM L53K12

TECH LIBRARY KAFB, NM
0144278


NACA

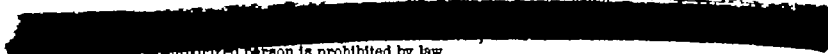
RESEARCH MEMORANDUM

A SUMMARY OF INFORMATION ON SUPPORT INTERFERENCE AT
TRANSONIC AND SUPERSONIC SPEEDS

By Eugene S. Love

Langley Aeronautical Laboratory
Langley Field, Va.

CLASSIFIED DOCUMENT


Unauthorized person is prohibited by law.

**NATIONAL ADVISORY COMMITTEE
FOR AERONAUTICS**

WASHINGTON
January 12, 1954





7502

Classification permitted (or changed to) CONFIDENTIAL

By 100 **NASA Technical Information Administration**

ON AUTHORIZED TO CHANGE

By.....

89 8 Sept 00

GRADE OF OFFICIAL 100

100
DATE



NATIONAL ADVISORY COMMITTEE FOR AERONAUTICS

RESEARCH MEMORANDUM

A SUMMARY OF INFORMATION ON SUPPORT INTERFERENCE AT
TRANSONIC AND SUPERSONIC SPEEDS

By Eugene S. Love

SUMMARY

A compilation has been made of available information on the problem of support interference at transonic and supersonic speeds. This compilation indicates that at supersonic speeds there are sufficient experimental data to design properly sting supports and shrouds having negligible interference. At transonic speeds the interference problem becomes most acute, and more experimental information is needed.

INTRODUCTION

As a result of difficulties encountered in wind-tunnel investigations of particular aircraft configurations at transonic and supersonic speeds and the ensuing evaluation of these difficulties, the general availability of existing information on sting support and shroud interference was found to be lacking. Much of the published information on the problem of support interference is obscured under report headings that refer, and properly so, to the primary investigation and is therefore difficult to locate. Furthermore, some of the valuable existing information has, as yet, been unpublished and is at the disposal of only a few experimenters or test facilities. The purpose of this paper is to bring together most of the information that could be found in the belief that such a summary would be of value in the design of supports having small interference. In addition, this summary might also serve as a basis toward further study of support interference.

SYMBOLS

M Mach number
D diameter of base of test model

| | |
|----------|---------------------------------------------------------------|
| d | sting diameter |
| l | length of sting having constant diameter (measured from base) |
| θ | semiapex angle of conical shroud |
| β | boattail angle at base of test model |
| P_B | base pressure coefficient |
| R | Reynolds number (based on model length) |
| x | moment arm |
| C_D | total drag coefficient |
| C_m | pitching-moment coefficient |
| C_L | lift coefficient |
| P_B | base pressure |
| p_s | free-stream static pressure |
| L | body length |
| α | angle of attack |
| S | reference area |
| q | dynamic pressure |
| η | scale factor |
| Z | section modulus |
| f | bending stress |
| m | bending moment |
| F | force normal to sting axis |
| C_F | force coefficient, F/qS |

DISCUSSION

In the discussion to follow, any previously unpublished data will be presented without reference. The data which have been published will be presented with a minimum of detail and the reader may consult the associated reference if additional information is desired. During the compilation of this summary, numerous discussions were made with personnel of the three NACA laboratories, in particular of the Langley laboratory, and with a few representatives of industry. Any general opinions expressed are a result of these discussions or related correspondence.

Supersonic Speeds

Interference at zero angle of attack.— Perhaps the best known of the earlier investigations of support interference at supersonic speeds is that of Perkins (ref. 1). Tests were made at $M = 1.5$ of two bodies of revolution at $\alpha = 0^\circ$, one with a cylindrical afterbody and one having a boattail base. The investigation covered both laminar and turbulent boundary layers for variations in R from 0.6×10^6 to 5×10^6 . Results for the model having a cylindrical afterbody are shown in figure 1. (The curve for $R = 0.5 \times 10^6$ in the upper left-hand plot has been added from minor extrapolations to curves given in ref. 1.) The important part that Reynolds number plays in support interference when the flow ahead of the base is laminar is well illustrated and points up the necessity for knowledge of the factors affecting wake transition. When the boundary layer is turbulent ahead of the base, effects of Reynolds number are reduced noticeably. Results for the model having appreciable boattailing ($\beta \approx 14^\circ$) are not included herein, but in general, the effects of support length and support diameter were negligible for both laminar and turbulent boundary layers as long as the support length was equal to or greater than 1.7 body diameters and the support diameter was equal to or less than 0.4 body diameter.

Chapman, in reference 2, has presented results at $M = 1.5, 2.0$, and 2.9 of the effects of sting length and diameter upon P_B for several configurations for laminar and turbulent boundary layers. These results are shown in figure 2. From these data, the critical value of $\frac{l}{D}$ is seen to lie between 2 and 3. Also the desirability of not exceeding about 0.4 in $\frac{d}{D}$ is evident.

An investigation at $M = 1.62, 1.93$, and 2.41 of the effect of support diameter for several finned body configurations is reported in reference 3. For these tests, the fins supported the models and were

CONFIDENTIAL

LAC 57-257

8 percent thick with 45° sweepback; body fineness ratio was 9.17. The results are shown in figure 3. In all cases the boundary layer was turbulent ahead of the base and $\frac{l}{D}$ was always greater than 6. Other tests reported in reference 3 showed that, provided the boundary layer was turbulent, the fin effects upon P_B were small; therefore the sting interference for the bodies without fins may be assumed of the same order as that indicated in figure 3.

Reference 4 presents results for $M = 2.73$ to 4.98 which show the effects upon P_B of varying $\frac{d}{D}$ and $\frac{l}{D}$ for both laminar and turbulent boundary layers. All tests to determine the effects of $\frac{d}{D}$ were conducted with $\frac{l}{D} = 6$, and tests for effects of $\frac{l}{D}$ were made with $\frac{d}{D} = 0.375$. These data are shown in figure 4 and indicate no unusual trends or difference in critical values from those exhibited at the lower supersonic speeds. There remains some question as to whether the boundary layer was fully turbulent at $M = 4.98$ for the turbulent tests.

The results which have been presented thus far deal with the effects of $\frac{l}{D}$, $\frac{d}{D}$, body shape, and Reynolds number for supersonic speeds. These results permit the design of a reasonable sting that will have small interference if shroud effects are negligible. For structural reasons it is desirable that the value of $\frac{l}{D}$ be as small as possible, and, if a shroud is employed, such a condition brings the semiapex angle of the shroud θ into consideration. External balance housings and other devices for positioning the model often require shrouds of appreciable apex angle. Further, the loads on a model sometimes dictate that a tapered sting must be used to gain strength. It is important, therefore, to know the effect of varying shroud angle and whether or not stings of small taper may be used without creating interference if $\frac{d}{D}$ is subcritical. The results of an investigation of this type made by August F. Bromm in the Langley 9-inch supersonic tunnel are shown in figure 5 for $M = 1.62$, 1.93 , and 2.41 . All results are for $\frac{d}{D} = 0.33$ and for a turbulent boundary layer with $R = 2.5 \times 10^6$. (It has been found that when the boundary layer is turbulent, changes in Reynolds number have only small effect upon the magnitude of the interference; see fig. 1, for example.) The data of figure 5 show that in this Mach number range a tapered sting ($\frac{l}{D} = 0$) must have a taper angle less than 2.5° to eliminate interference, even though $\frac{d}{D}$ exactly at the base is

subcritical. Another result of these tests is that the critical value of $\frac{l}{D}$ for a given Mach number is essentially independent of θ for values of θ at least up to 20° ; this factor aids considerably in the design of the sting-shroud combination. A comparison of the data for the three Mach numbers shows that the critical value of $\frac{l}{D}$ decreases slightly with increasing Mach number: from about 2.25 at $M = 1.62$ to about 2 at $M = 2.41$. From reference 5, the distance from the base of the body to the base of the trailing shock in terms of $\frac{l}{D}$ is also seen to decrease with increasing M ; further the critical $\frac{l}{D}$ values for shroud location are seen to correspond approximately to positions 0.85 base diameters downstream of the base of the trailing shock. The addition of 0.85 to the curve of figure 36 in reference 5 may, therefore, serve as a tentative guide in establishing critical $\frac{l}{D}$ values for shrouds having θ no greater than 20° . Such a procedure indicates that at low supersonic Mach numbers a large increase in $\frac{l}{D}$ critical is to be expected.

Figure 6 presents results obtained in the Langley 4- by 4-foot supersonic tunnel at $M = 1.59$ for the NACA RM-10 missile body, which is a parabolic body of fineness ratio 12.2. Here again the critical value of $\frac{l}{D}$ is seen to be relatively independent of θ for values up to 20° in spite of the fact that all the values of $\frac{d}{D}$ are supercritical (left-hand plot). In the right-hand plot are data showing effects of $\frac{d}{D}$ for laminar flow. As mentioned previously, an understanding of wake transition is necessary before proper interpretation can be made for laminar flow.

Interference at angle of attack.- Reference 6 presents some results of the variation of $\frac{d}{D}$ and θ on the lift, drag, and pitching moment of a finned model of the NACA RM-10 missile at $M = 1.62$. A sketch of the model is shown in figure 7(a). The value of $\frac{l}{D}$ was held constant at 2.72, and the boundary layer was turbulent. The results showed that increasing $\frac{d}{D}$ from 0.715 to 0.992 (both supercritical) gave greater non-linearity in the lift and pitching-moment curves, decreased the lift-curve slope through zero lift by about 7 percent, increased the pitching-moment curve slope through zero lift by about 10 percent (less negative), and reduced the fore drag at zero lift by approximately 10 percent. Because of structural limitations, the tests at $\frac{d}{D} = 0.489$ were confined

to $\alpha = 0^\circ$. (An external balance was employed in these tests, and d corresponds to the outside diameter of the cylindrical portion of the sting shield. The actual diameter of the sting is, of course, much smaller.)

Figure 7(b) presents a sketch of a model of the X-2 airplane which was tested in the Langley 4- by 4-foot supersonic tunnel at $M = 1.6$ for $\alpha = 0^\circ$ to 10° . The quarter chord of the horizontal stabilizer of this model is swept back 41° . For these tests the boundary layer ahead of the base was turbulent. The model was tested with various bent stings at angles of 0° , 3° , and $\pm 6^\circ$. (See fig. 7(b).) The results showed that bending the sting had negligible effect upon the lift, drag, pitching moment, and stabilizer hinge moment. However, the fact that the bent stings had no effect does not obviate the condition that both $\frac{d}{D}$ and $\frac{L}{D}$ were supercritical.

Results are available from tests in the Langley 9-inch supersonic tunnel to determine the interference at large α of a sting designed to have small interference at $\alpha = 0^\circ$. These tests were made with a body of fineness ratio 9.3 having a cylindrical afterbody and parabolic nose and mounted to the tunnel side wall by means of a shielded trunnion. This installation permitted the model to be rotated through 360° in the center of the test section and in a plane parallel to the tunnel side walls. (Shield was fixed to tunnel wall and did not rotate.) A length of sting having a value of $\frac{d}{D} = 0.357$, and sufficiently long to extend beyond the base of the trailing shock, could be inserted in the hollow base of the body. The results of these tests are shown in figure 8. It should be emphasized that the absolute magnitude of P_B has little significance because of the effects the trunnion shield may have upon P_B ; however, for the assessment of sting interference, these effects from the trunnion shield are of no concern, since the pressure field which the shield creates in the vicinity of the base at any value of α is obviously the same with and without sting. At $M = 1.62$ no data are shown beyond $\alpha = 40^\circ$, since reflected shocks appeared to intersect the wake close to the base. For the same reason, the values from $\alpha = 20^\circ$ upward should be viewed with some caution. At $M = 1.93$ and 2.41 , all the data are reliable and free of reflected shocks. It is clear from these results that sting supports so designed to have small effect upon P_B at $\alpha = 0^\circ$ may be expected to have equally small effects at values of α up to 60° . The same would probably apply at $M = 1.62$.

Transonic Speeds

Consideration will now be given to information at transonic speeds. In figure 9 are presented results from free-flight tests reported in

reference 7. These tests were made with a finless body of fineness ratio 11. A turbulent boundary layer existed ahead of the base. The large amount of sting interference that occurs in the transonic speed range is clearly indicated. Of the available information at transonic speeds, only these data (no sting) offer a basis for assessing wind-tunnel results and the magnitude of interference without fin effects.

Figure 10 presents some results obtained in the Langley 8-foot transonic tunnel for a body nearly parabolic in shape and having a fineness ratio of about 10. (See ref. 8.) Also shown are results obtained by the Pilotless Aircraft Research Division in free flight of a similar model, but having three fins, in an effort to shed some light on the sting-interference problem at transonic speeds. It will be noted (fig. 10) that both $\frac{d}{D}$ and $\frac{l}{D}$ are supercritical for supersonic speeds and would be more so in the transonic range. Nevertheless, the free-flight results do serve to show the large interference from such a sting installation. The difference between the free-flight and wind-tunnel results with sting is apparently due to the presence of the fins on the free-flight model.

Recently, the staff of the Ames 2- by 2-foot transonic tunnel has been conducting a rather extensive program to study the model support problem. Figure 11 presents results obtained in this facility at $R \approx 6.2 \times 10^6$ (turbulent boundary layer). The configuration consisted of a body with wing (see sketch, fig. 11). The body had a fineness ratio of 9.9 and was slightly boattailed. The wing had a 3-percent-thick biconvex section, an aspect ratio of 3.09, and a taper ratio of 0.39.

It is obvious that the value of $\frac{d}{D} = 0.961$ is highly supercritical, but the results give considerable insight into the extreme difficulties confronting experimenters in the high subsonic and transonic speed range. The critical value of $\frac{l}{D}$ for this particular value of $\frac{d}{D}$ does not appear to be reached except at $M \geq 1.1$. Application of these results to other values of $\frac{d}{D}$ should be made with caution, since for subcritical values of $\frac{d}{D}$, the critical value of $\frac{l}{D}$ indicated for $M \geq 1.1$ would be too small.

In reference 9, an investigation has been made at transonic speeds of the effect of $\frac{d}{D}$ upon the lift, drag, pitching moment, and base pressure of a model of the D-558-II airplane. These results are shown in figure 12. All stings utilized in obtaining these results had taper of the order of 2° to 4° with $\frac{l}{D} = 0$. Extrapolation of the results to $\frac{d}{D} = 0$ would be rather broad in any event, and in view of the results presented in figures 9 and 10 such an extrapolation would lead to

considerable error in base drag. Whether or not extrapolative procedures may be used in the transonic range awaits further experimental work.

Other Information

Experimental results.- In reference 10 some effects of support interference at high subsonic speeds are reported. In view of what is now known concerning the relation of model size to slotted test section size, use of the data of reference 10 would appear limited. Reference 11 presents information on support interference at supersonic speeds with emphasis upon windshield design from the standpoint of best tunnel design. In reference 12 an experimental investigation was performed to determine the effect on base and forebody pressures of using a sting modified with varying length splitter plates and fins, instead of conventional sting, to support a cone-cylinder body of revolution. The investigation was conducted at $M = 3.12$ for R ranging from 2×10^6 to 14×10^6 and for values of α from 0° to 9° . Results indicated that for $R = 8 \times 10^6$ and 14×10^6 there was negligible effect of the splitter plate modification on base pressure and at $R = 2 \times 10^6$ there was a small effect. Positioning the leading edge of the splitter plate at or ahead of the base made no appreciable change in the influence of the modifications on base pressure at $R = 14 \times 10^6$. With the fin-type modification there was a small increase in base pressure. The same general configuration was tested at $M = 1.91$ and reported in reference 13 where the pressure upstream of the base varied in accordance with exact potential flow theory at zero angle of attack. The pressures were slightly higher as was expected due to the presence of body boundary layer. In the investigation of a strut-supported 16-inch ram jet at $M = 1.5$ to 2.0 reported in reference 14, a dummy strut (identical to the original in every way) was attached to the tunnel wall with approximately 3/16-inch clearance maintained between the strut and the model. It was found that the interference drag could not be measured by the tunnel scales and was therefore assumed to be negligible. The dummy strut was then detached from the tunnel wall and attached to the tunnel scale so the drag of the model and two struts could be measured. Subtracting the drag value for the model and supporting strut gave the drag of a single strut and hence model drag could be calculated.

There are scattered bits of information and results of minor investigations available that have not been mentioned herein. These have been omitted since they are either covered by the data which are included or because certain of the variables were so highly supercritical that the results were of little value.

General comments.- In the process of gathering material for this summary, it was observed that there was a very noticeable tendency toward "overdesign" of sting size as model size is increased which could not be attributed to dead-weight requirements. If a given small-scale model with subcritical sting size may be tested without fear of failure, increasing the sting size out of proportion to the increase in model scale cannot be justified. This may be shown simply. Assume that a force F normal to the sting axis is the primary load upon the sting and that it acts through a moment arm x . The bending moment m produced is

$$m = Fx = (C_F q S) x \quad (1)$$

At a larger scale factor η ,

$$m_\eta = F_\eta x_\eta = \eta^2 (C_F q S) \eta x = \eta^3 m \quad (2)$$

since the area of the model increases as the square of the scale factor and the $\frac{l}{D}$ ratio is held constant. If a solid sting of circular cross section is used, the bending stress is

$$r = \frac{m}{Z} = \left(\frac{32}{\pi} \right) \frac{m}{d^3} \quad (3)$$

At a larger scale factor η

$$r_\eta = \left(\frac{32}{\pi} \right) \frac{m_\eta}{(d_\eta)^3} = \left(\frac{32}{\pi} \right) \frac{\eta^3 m}{\eta^3 d^3} = \left(\frac{32}{\pi} \right) \frac{m}{d^3} \quad (4)$$

since the $\frac{d}{D}$ ratio is held constant.

Thus, the stress is seen to be unaffected by scale factor. Quite often the larger scale models operate at reduced q as compared with the smaller scale models; if so, the larger models gain in relative sting strength.

For the prevention of sting failure caused by the buffeting that accompanies starting in supersonic tunnels, several methods are commonly employed: for example, lowering the density of the air during starting (closed circuit tunnels) and the use of various temporary struts to brace the model during the starting cycle after which the struts are withdrawn. In transonic tunnels, buffeting may remain after the starting cycle. This feature, coupled with the indication that in the transonic speed range subcritical values of $\frac{d}{D}$ and $\frac{l}{D}$ may approach absurd magnitudes, would appear to raise doubt that it will be possible to make interference-free measurements in this speed range. This would apply particularly to base drag and factors affecting it, such as fin design and location. At this time, most transonic experimenters appear to feel that, with judicious support design, interference effects upon lift and pitching moment may be reduced to negligible quantities at the sacrifice of measuring realistic base drag (base pressure is corrected to some appropriate level such as stream static or replaced by a reasonable estimate).

CONCLUDING REMARKS

A summary has been prepared of available information on the support-interference problem at transonic and supersonic speeds. The compilation of experimental data indicates that at supersonic speeds the design criteria for sting supports and shrouds are fairly well established. At transonic speeds the problem becomes most acute, and more information is needed in this speed range.

Langley Aeronautical Laboratory,
National Advisory Committee for Aeronautics,
Langley Field, Va., October 27, 1953.

REFERENCES

1. Perkins, Edward W.: Experimental Investigation of the Effects of Support Interference on the Drag of Bodies of Revolution at a Mach Number of 1.5. NACA TN 2292, 1951.
2. Chapman, Dean R.: An Analysis of Base Pressure at Supersonic Velocities and Comparison with Experiment. NACA TN 2137, 1950.
3. Love, Eugene S., and O'Donnell, Robert M.: Investigations at Supersonic Speeds of the Base Pressure on Bodies of Revolution with and without Sweptback Stabilizing Fins. NACA RM L52J21a, 1952.
4. Reller, John O., Jr., and Hamaker, Frank M.: An Experimental Investigation of the Base Pressure Characteristics of Nonlifting Bodies of Revolution at Mach Numbers from 2.73 to 4.98. NACA RM A52E20, 1952.
5. Love, Eugene S.: The Base Pressure at Supersonic Speeds on Two-Dimensional Airfoils and Bodies of Revolution (With and Without Fins) Having Turbulent Boundary Layers. NACA RM L53C02, 1953.
6. Coletti, Donald E.: Investigation of the Aerodynamic Characteristics of the NACA RM-10 Missile (with Fins) at a Mach Number of 1.62 in the Langley 9-inch Supersonic Tunnel. NACA RM L52J23a, 1952.
7. Hart, Roger G.: Effects of Stabilizing Fins and a Rear-Support Sting on the Base Pressure of a Body of Revolution in Free Flight at Mach Numbers from 0.7 to 1.3. NACA RM L52E06, 1952.
8. Osborne, Robert S., and Mugler, John P., Jr.: Aerodynamic Characteristics of a 45° Sweptback Wing-Fuselage Combination and the Fuselage Alone Obtained in the Langley 8-Foot Transonic Tunnel. NACA RM L52E14, 1952.
9. Osborne, Robert S.: High-Speed Wind-Tunnel Investigation of the Longitudinal Stability and Control Characteristics of a 1/16-Scale Model of the D-558-2 Research Airplane at High Subsonic Mach Numbers and at a Mach Number of 1.2. NACA RM L9C04, 1949.
10. Aldrich, J. F. L.: Some Sting Support Interference Effects in a Subsonic Slotted Test Section. USCAL 10-3-1 (Contract Noa(s) 10585-Item 3), Aeronautical Lab., Univ. of Southern Calif., May 31, 1951.
11. Puckett, Allen E.: Final Report on the Model Supersonic Wind-Tunnel Project. Armor and Ordnance Rep. No. A-269, OSRD No. 3569, NDRC. April, 1944.

12. Baughman, L. Eugene, and Jack, John R.: Experimental Investigation of the Effects of Support Interference on the Pressure Distribution of a Body of Revolution at a Mach Number of 3.12 and Reynolds Numbers from 2×10^6 to 14×10^6 . NACA RM E53E28, 1953.
13. Cortright, Edgar M., Jr., and Schroeder, Albert H.: Preliminary Investigation of Effectiveness of Base Bleed in Reducing Drag of Blunt-Base Bodies in Supersonic Stream. NACA RM E51A26, 1951.
14. Nussdorfer, T., Wilcox, F., and Perchonok, E.: Investigation at Zero Angle of Attack of a 16-Inch Ram-Jet Engine in 8- by 6-Foot Supersonic Wind Tunnel. NACA RM E50L04, 1951.

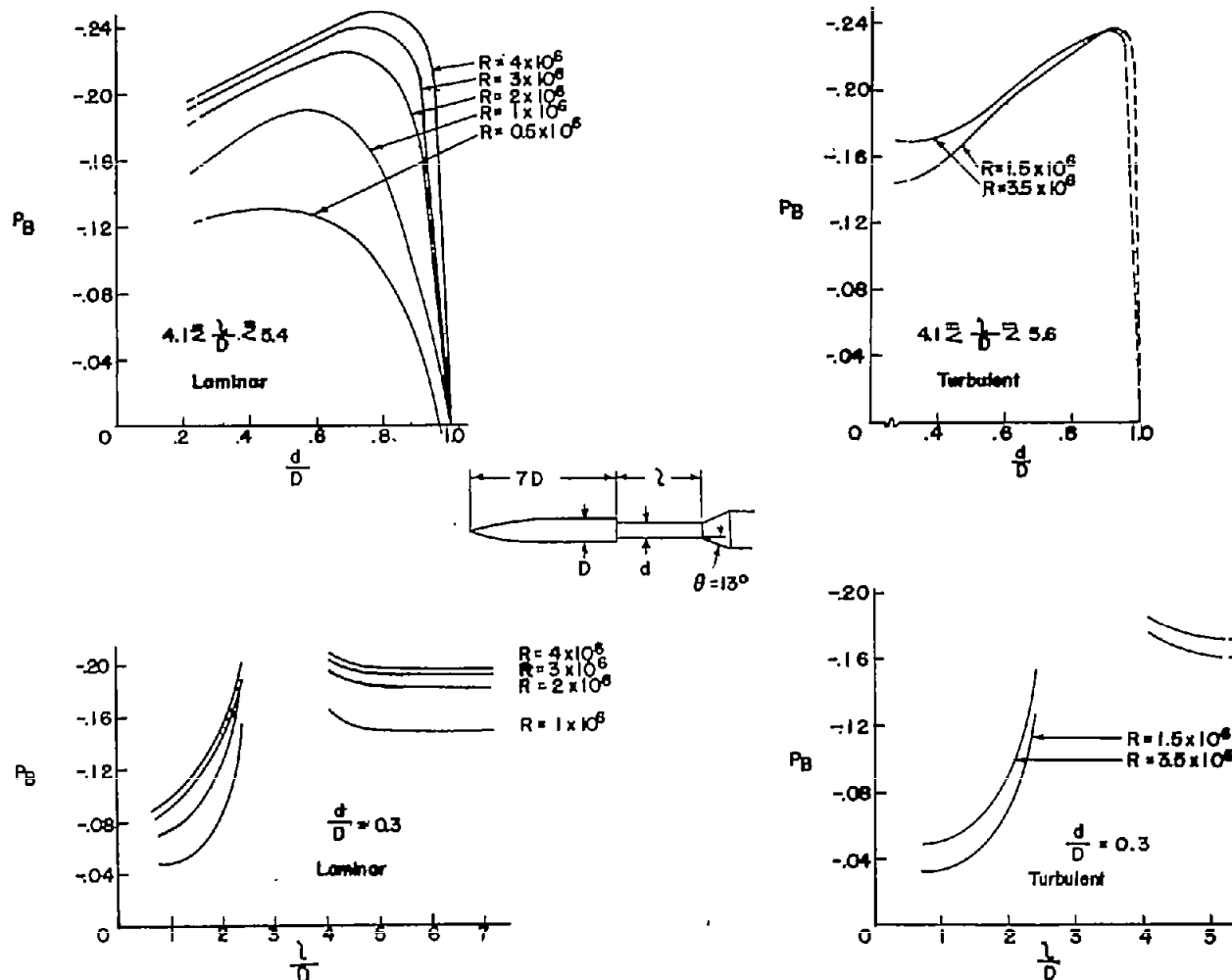


Figure 1.- Effects upon the base-pressure coefficient of the ratio of sting diameter to base diameter and of sting length to base diameter for laminar and turbulent boundary layers at $M = 1.5$.

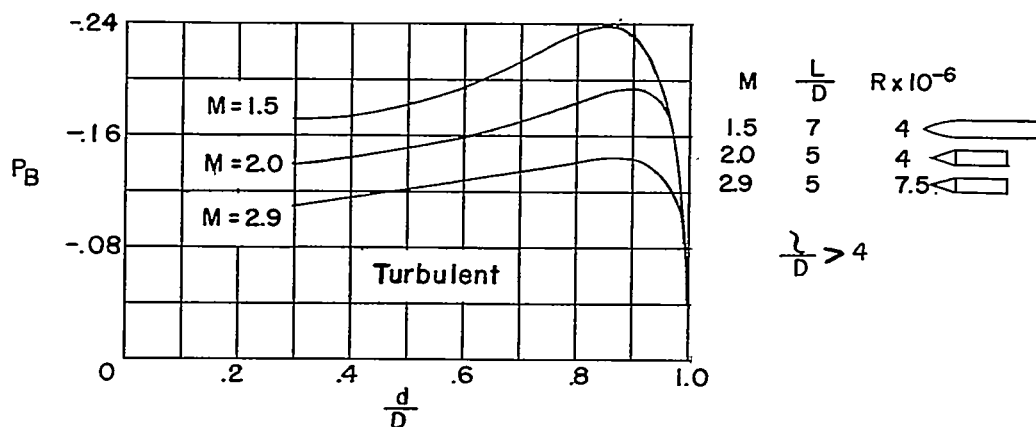
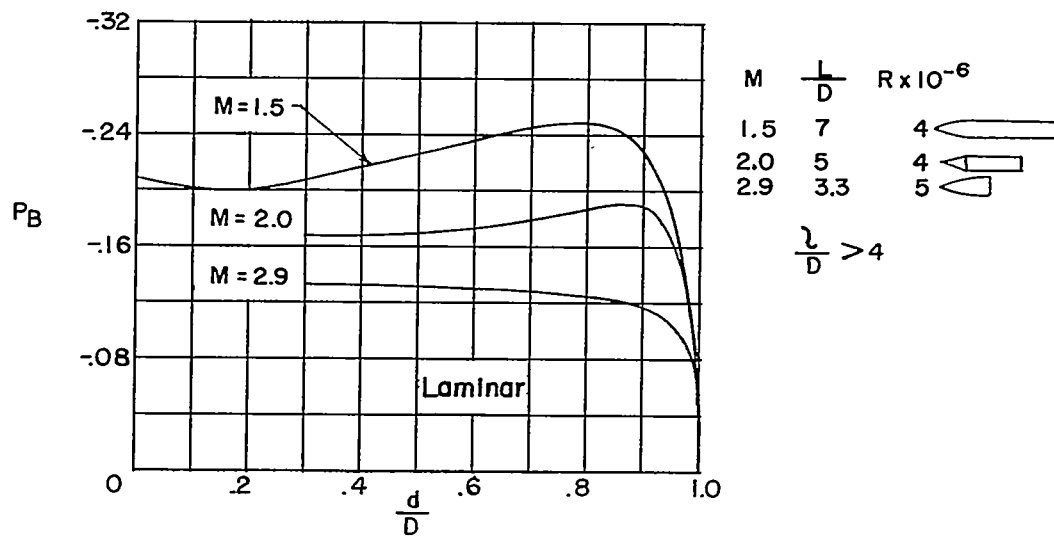
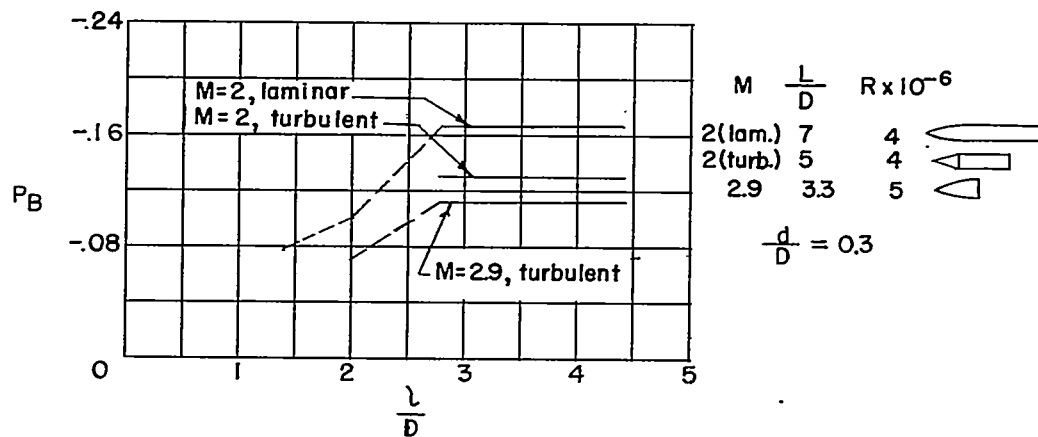


Figure 2.- Effects upon the base-pressure coefficient of the ratio of sting diameter to base diameter and of sting length to base diameter for laminar and turbulent boundary layers at $M=1.5$, $M=2.0$, and $M=2.9$.

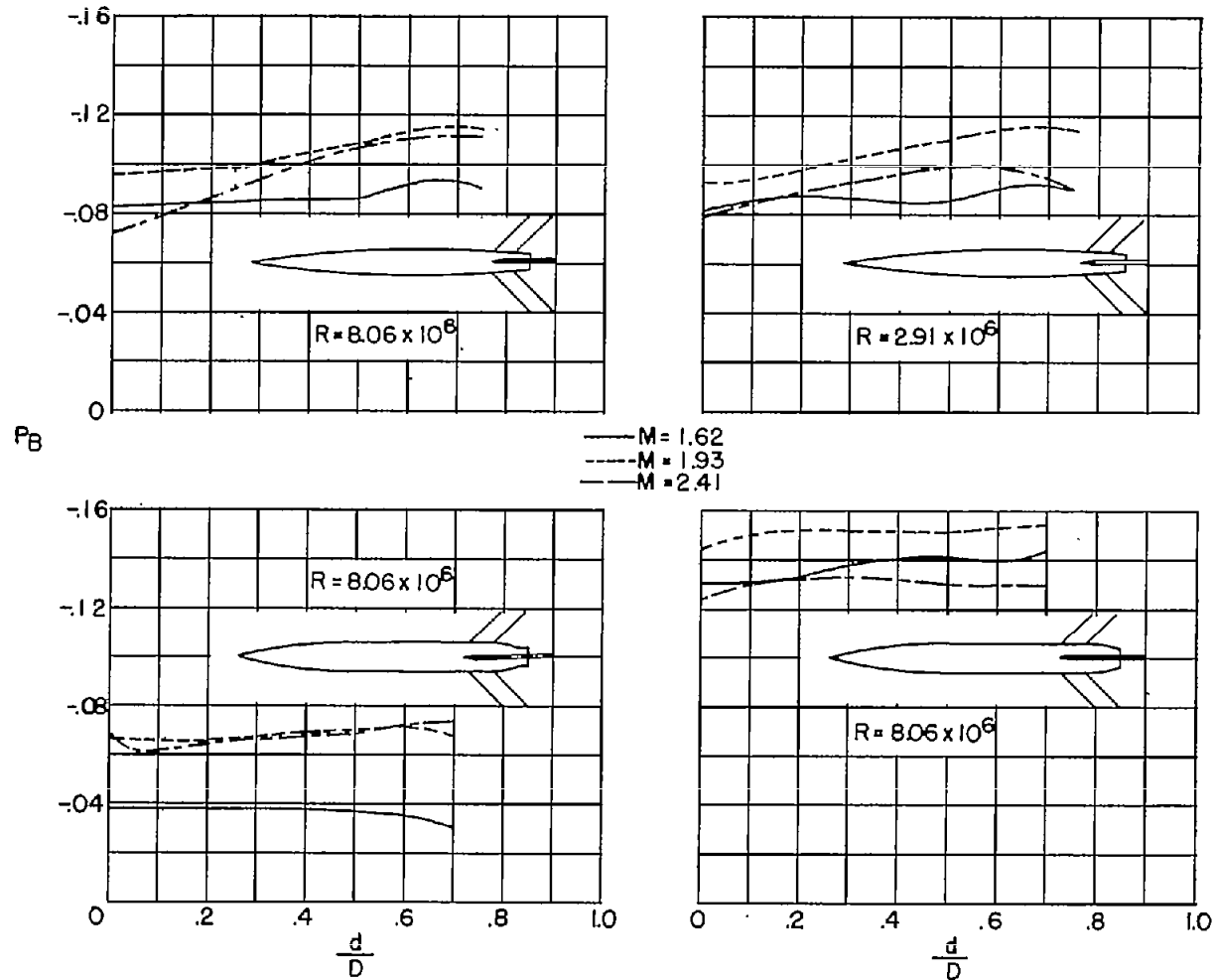


Figure 3.- Effects upon the base-pressure coefficient of the ratio of sting diameter to base diameter for several finned bodies at $M = 1.62$, 1.93 , and 2.41 . Turbulent boundary layer; $\frac{l}{D} > 6$.

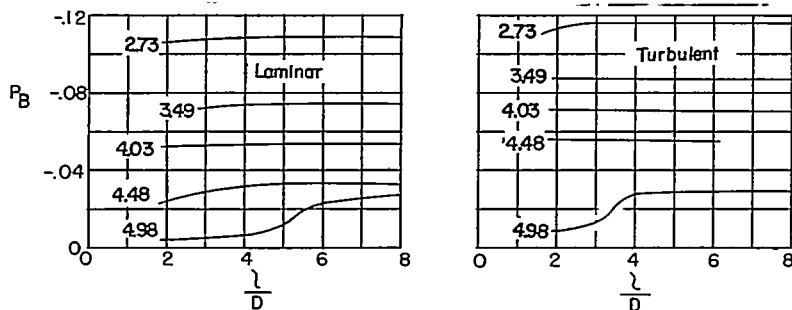
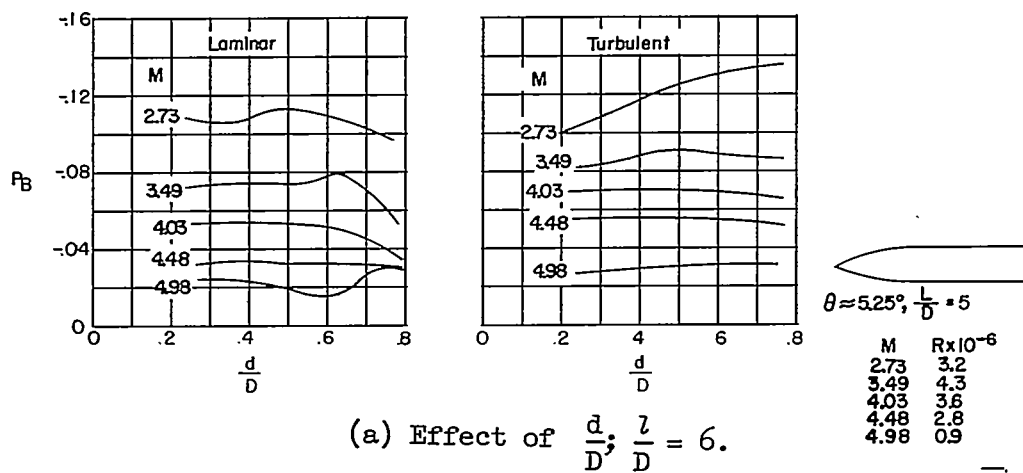


Figure 4.- Effects upon the base-pressure coefficient of the ratio of sting diameter to base diameter and of sting length to base diameter for laminar and turbulent boundary layers at $M = 2.73, 3.49, 4.03, 4.48, \text{ and } 4.98$.

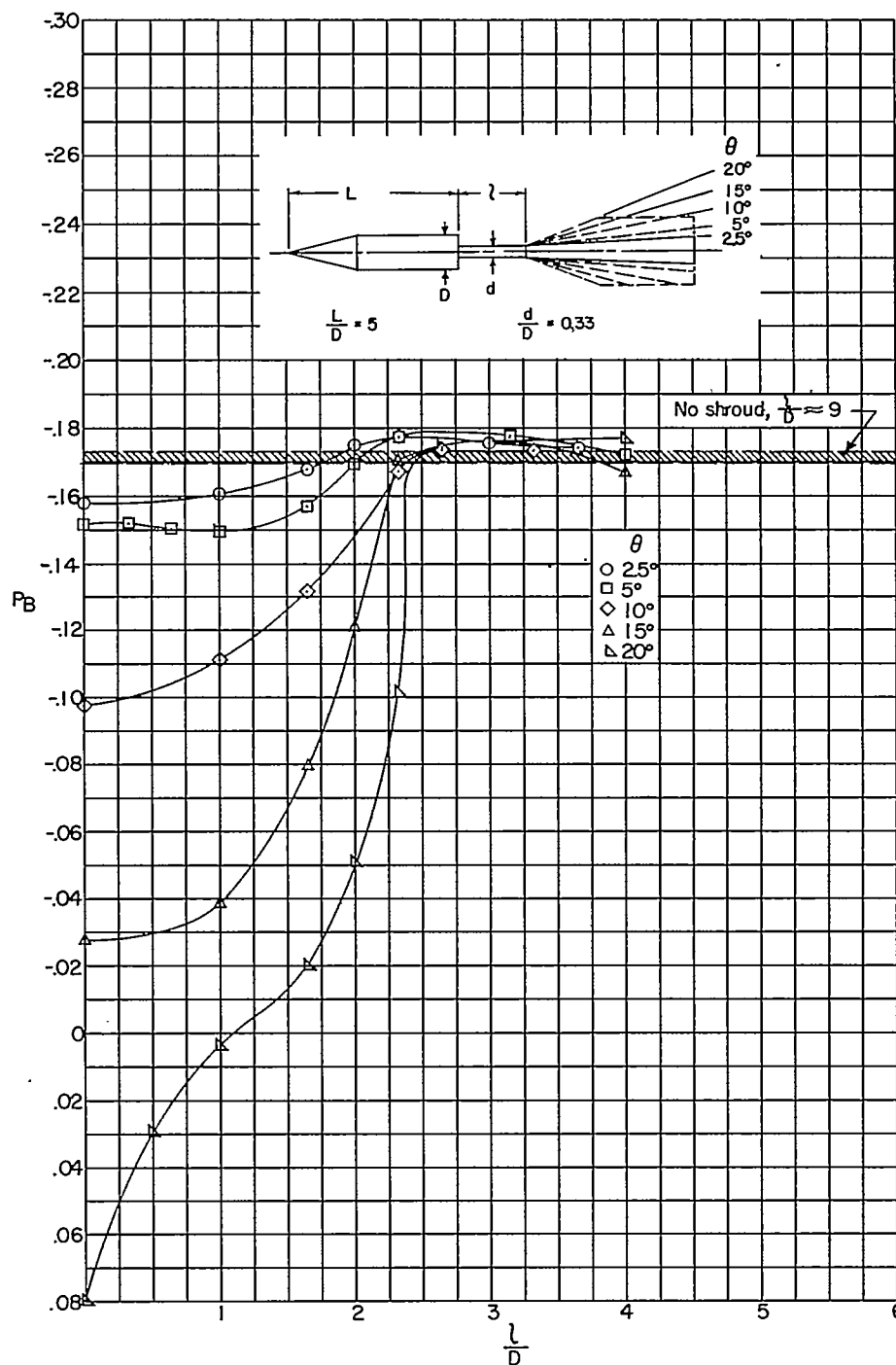
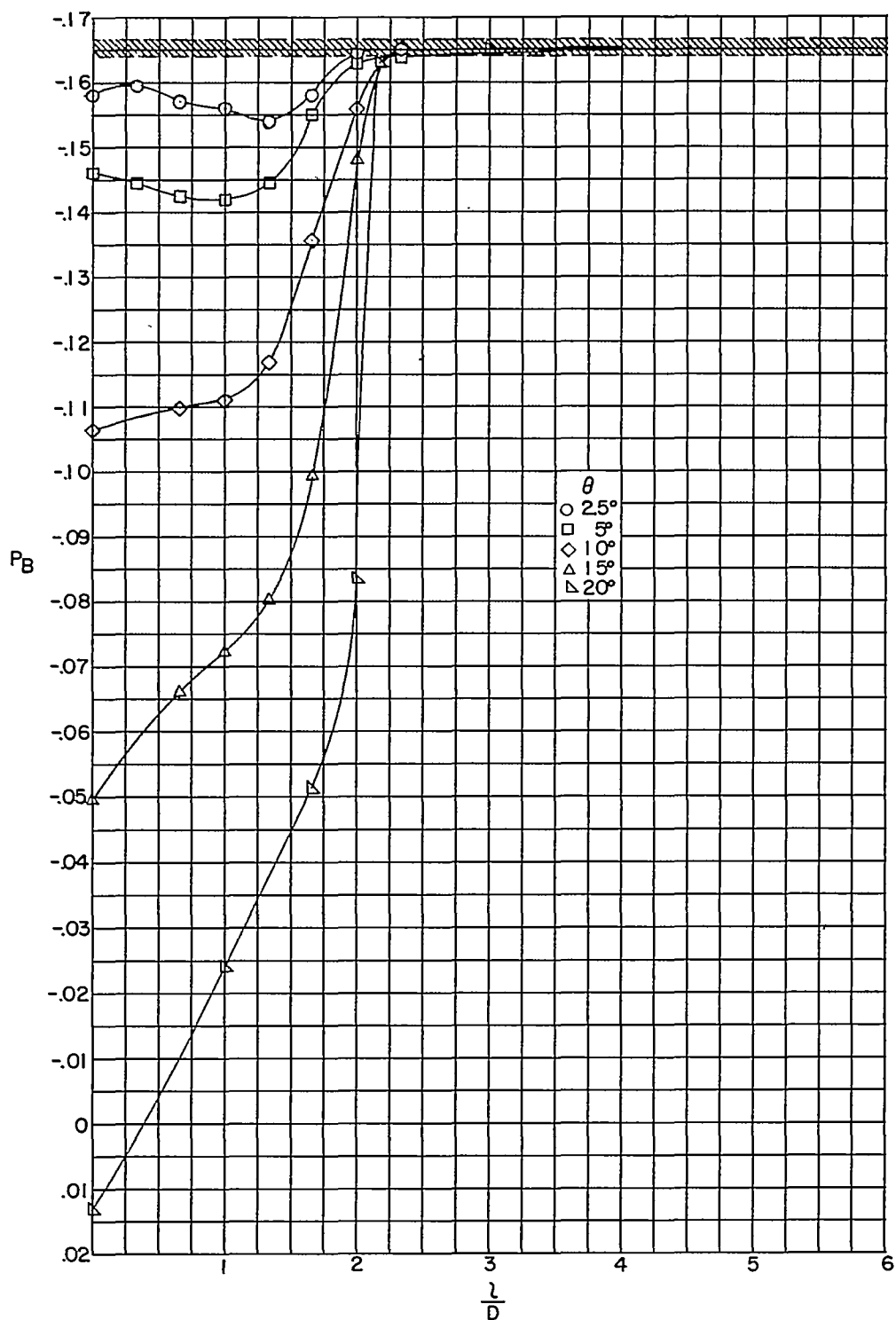
(a) $M = 1.62$.

Figure 5.- Effects upon the base-pressure coefficient of the ratio of shroud length to base diameter for various semiapex angles of a conical shroud. Turbulent boundary layer; $d/D = 0.33$.



(b) $M = 1.93$.

Figure 5.- Continued.

CONFIDENTIAL

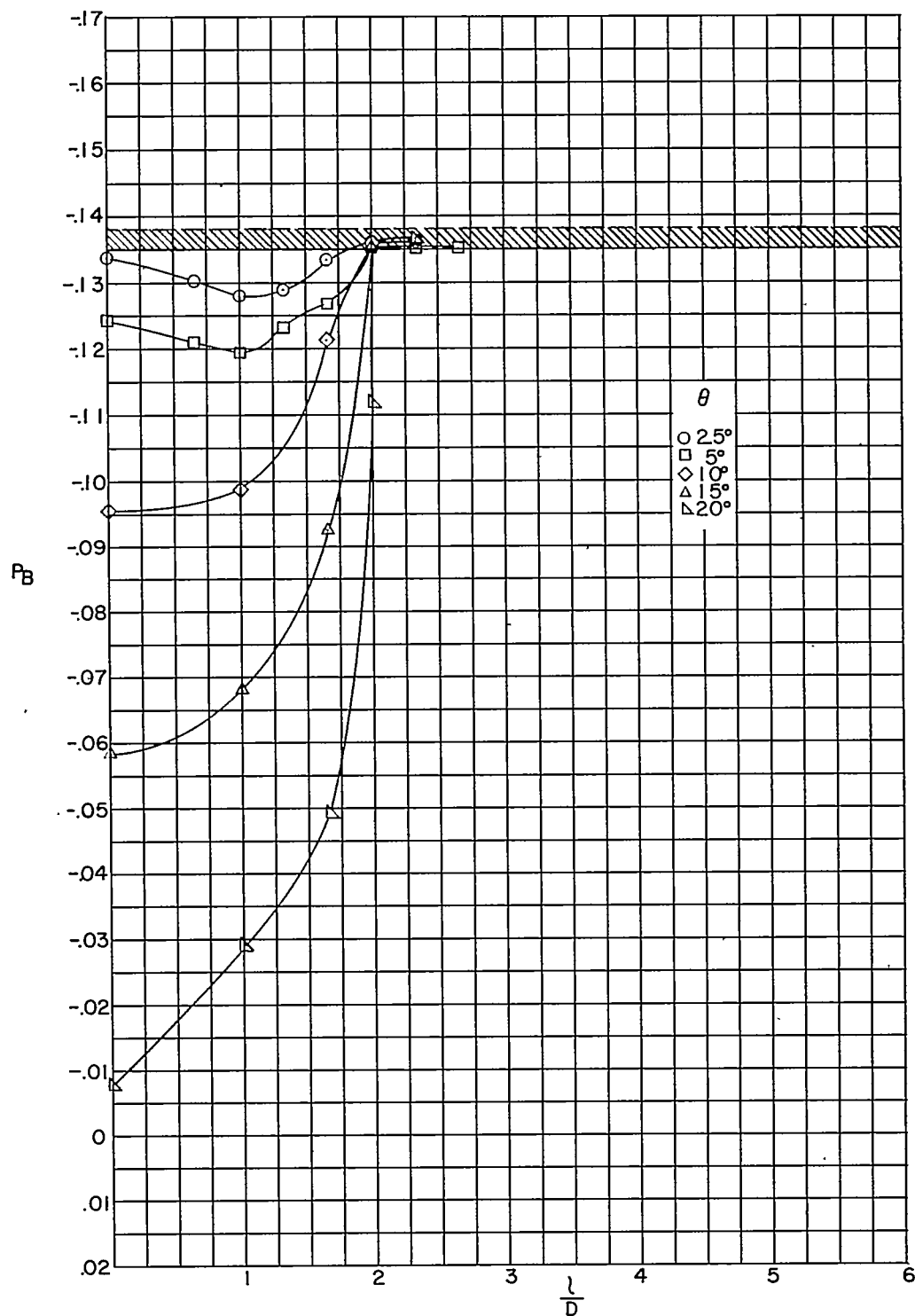
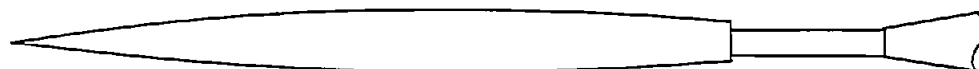
(c) $M = 2.41$.

Figure 5.- Concluded.

CONFIDENTIAL



$$\theta \begin{cases} \circ & 3^\circ \\ \square & 10^\circ \\ \diamond & 20^\circ \end{cases} \quad \frac{d}{D} \begin{cases} \text{—} & 0.60 \\ \text{---} & 0.78 \\ \text{- - -} & 1.00 \end{cases}$$

$$1.95 \leq \frac{l}{D} \leq 6.00$$

$$R \approx 4 \times 10^6$$

(No significant effects of $\frac{l}{D}$)

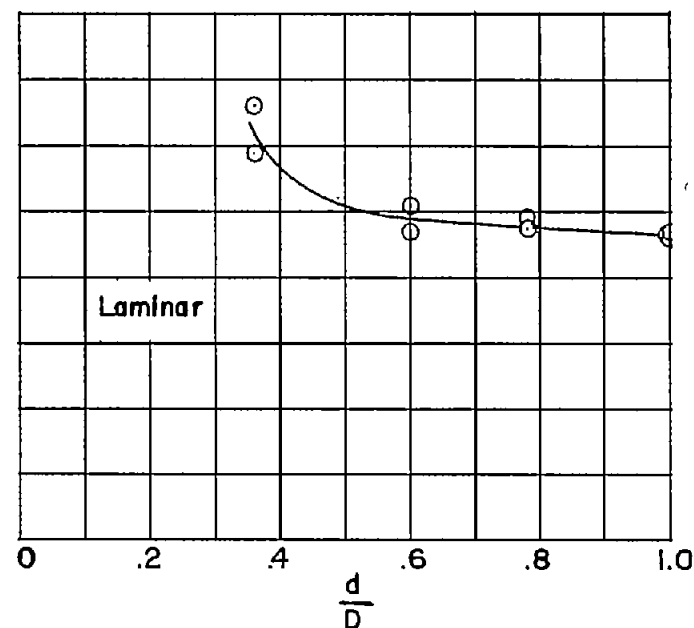
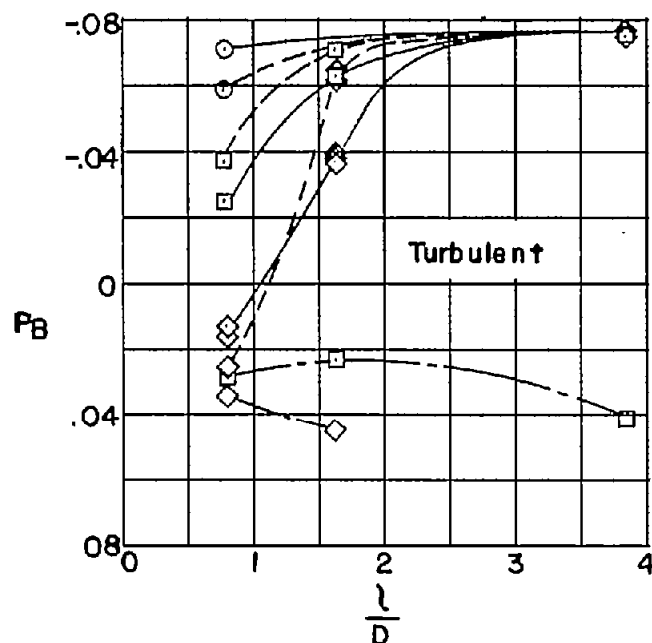
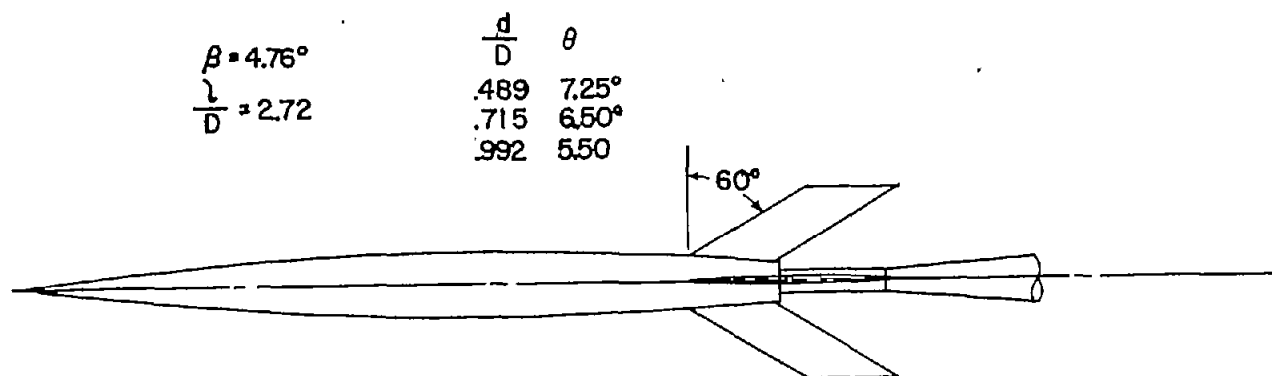


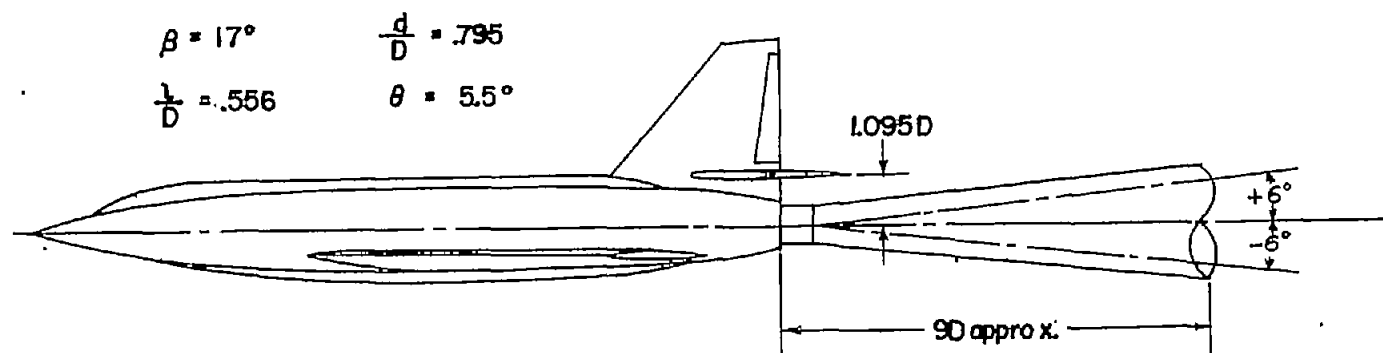
Figure 6.- Effects upon the base-pressure coefficient of the ratio of sting length to base diameter and semiapex angle of a conical shroud and of the ratio of sting diameter to base diameter for the NACA RM-10 missile at $M = 1.59$.

CONFIDENTIAL

CONFIDENTIAL



(a) NACA RM-10 missile.



(b) Model of X-2 airplane.

Figure 7.- Sketch of model configurations.

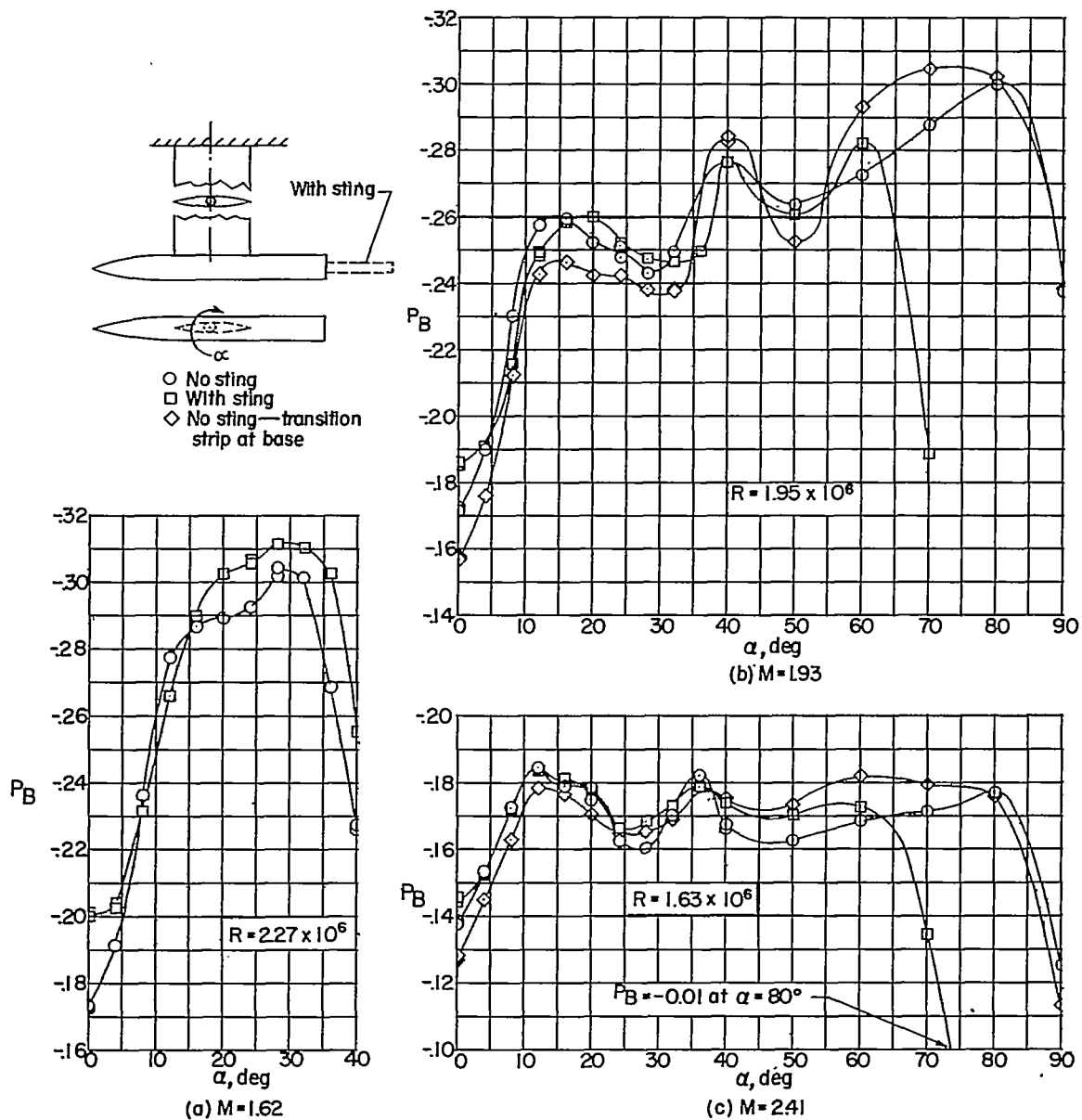


Figure 8.- Effects of a sting and of a transition strip at the rear of the body upon the base pressure at angle of attack.

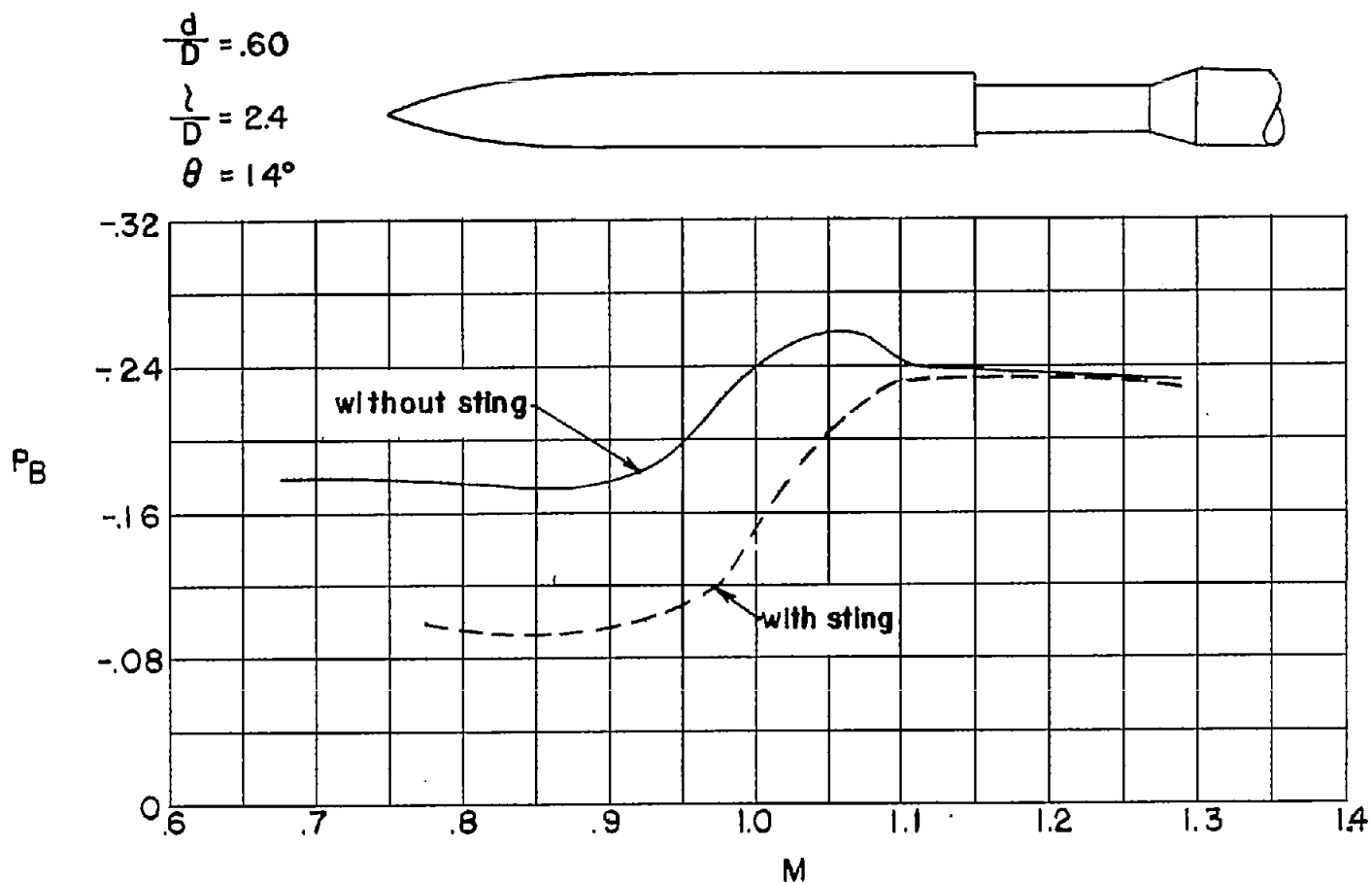


Figure 9.- Effects upon the base-pressure coefficient of a typical sting installation. (Free-flight results, turbulent boundary layer.)

CONFIDENTIAL

NACA RM L53K12

| | $\frac{d}{D}$ | $\frac{l}{D}$ | θ | Fins | β |
|-----------------------|---------------|---------------|----------|-------------|---------|
| Free flight (PARC) | 0.755 | 0.387 | 4.25° | 3-45° sweep | 5.7° |
| Wind tunnel (8° T.T.) | 0.755 | 0.387 | 3.9° | none | 5.7° |

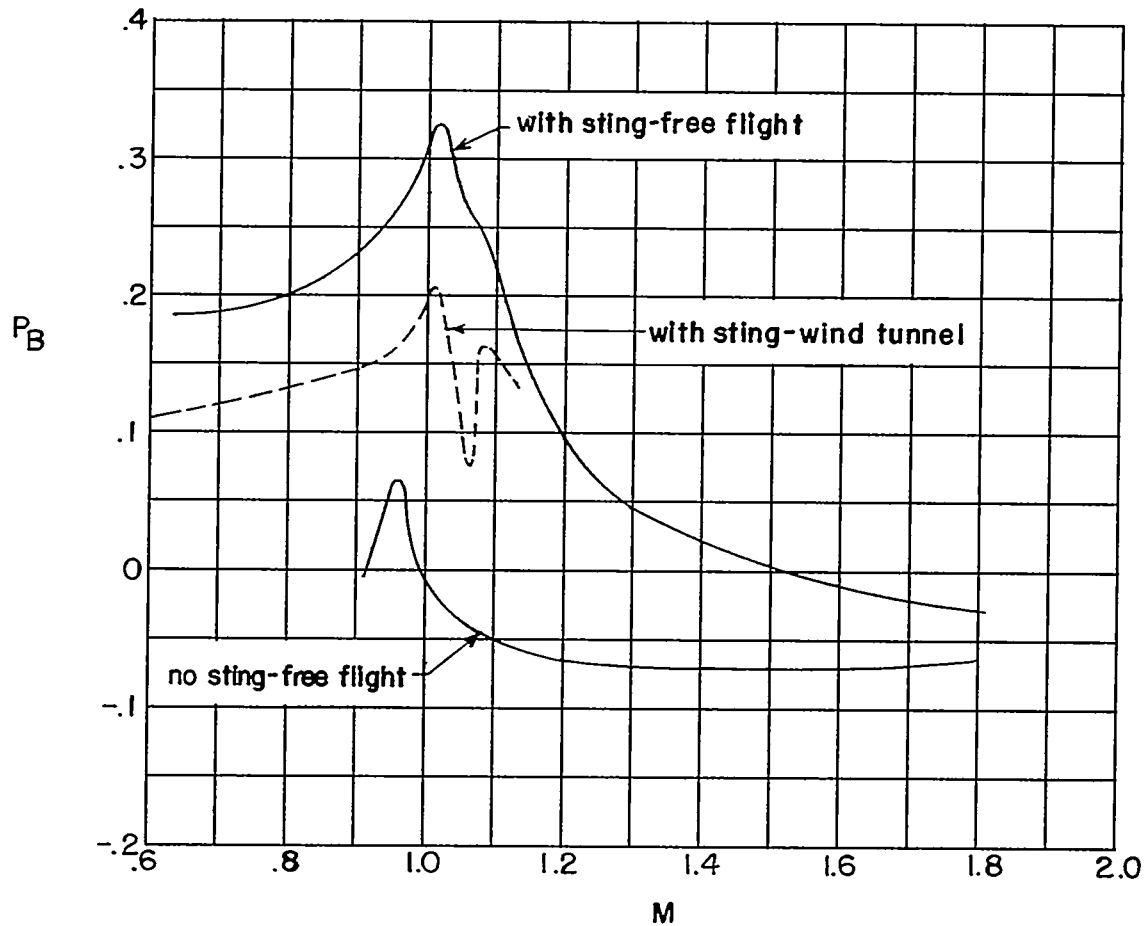


Figure 10.- Effects upon the base-pressure coefficient of a transonic sting installation on a finned missile in free flight. (Also comparison with unfinned wind-tunnel results.)

CONFIDENTIAL

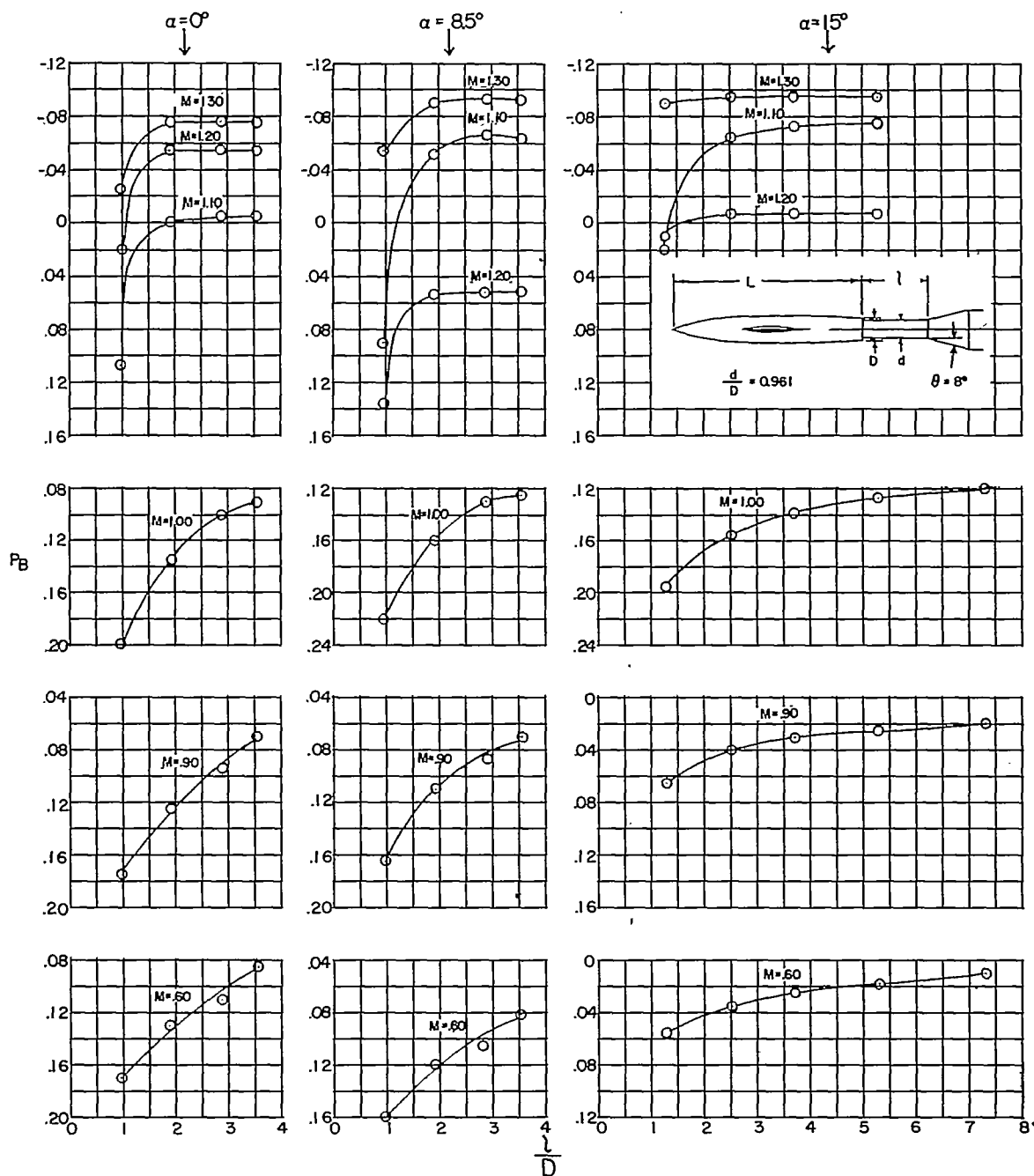


Figure 11.- Effects upon the base-pressure coefficient of the ratio of sting length to base diameter for $\alpha = 0^\circ$ to 15° and for $M = 0.60$ to 1.30 .

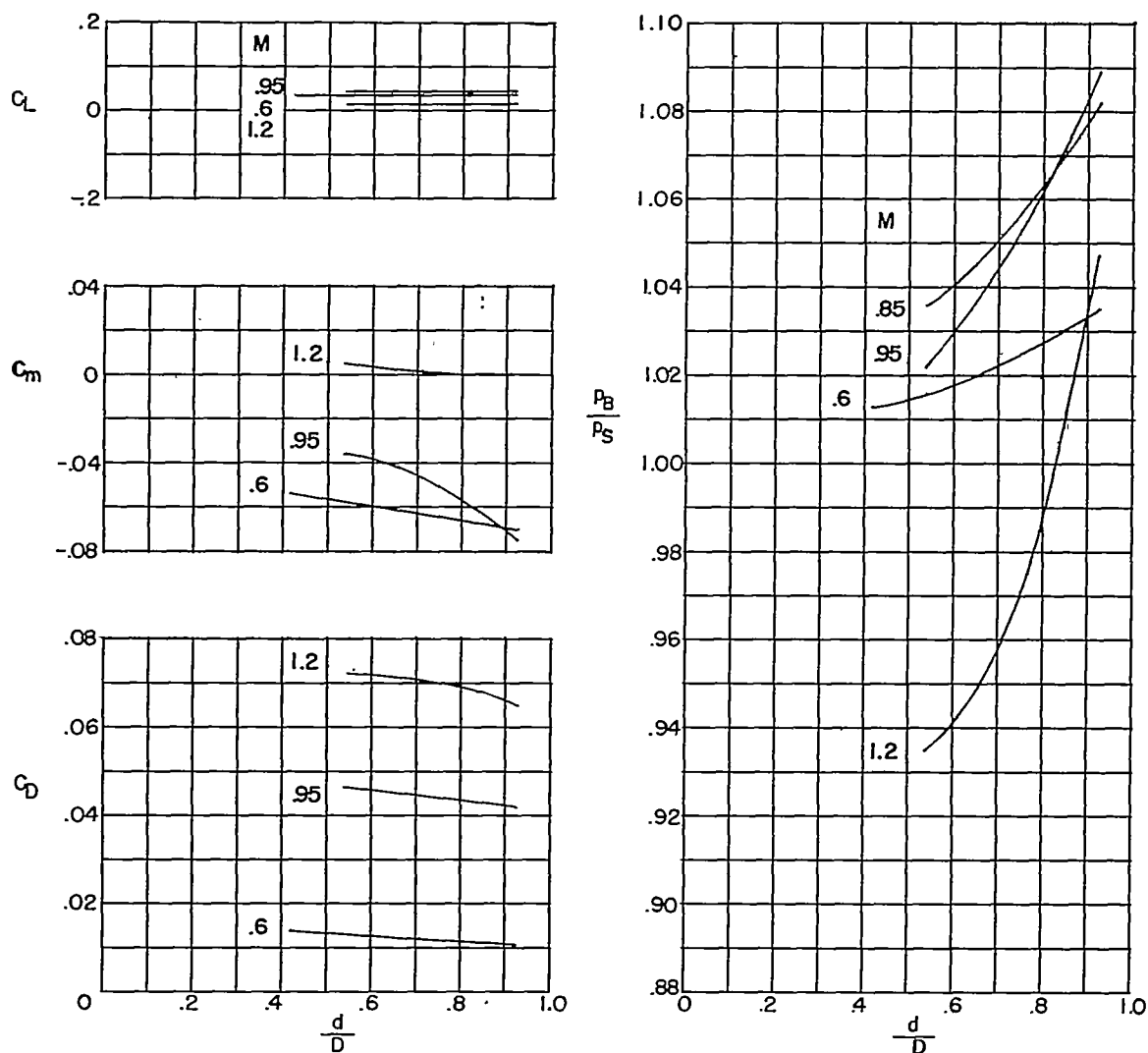


Figure 12.- Effects upon the force and base-pressure measurements of the ratio of sting diameter to base diameter for $M = 0.6$ to 1.2 . (D-558-II model; $\alpha = -2^\circ$; turbulent boundary layer. Tapered sting.)